Polyhedron 123 (2017) 404–410

Contents lists available at ScienceDirect

Polyhedron

journal homepage: www.elsevier.com/locate/poly

Exchange interaction between $S = 1/2$ centers bridged by multiple noncovalent interactions: Contribution of the individual chemical pathways to the magnetic coupling

Ana L. Pérez [a], Nicolás I. Neuman [a], Ricardo Baggio [b], Carlos A. Ramos [c], Sergio D. Dalosto [d], Alberto C. Rizzi [a], Carlos D. Brondino [a,*]

[a] Departamento de Física, Facultad de Bioquímica y Ciencias Biológicas, Universidad Nacional del Litoral – CONICET, Ciudad Universitaria, S3000ZAA Santa Fe, Argentina
[b] Gerencia de Investigación y Aplicaciones, Centro Atómico Constituyentes, Comisión Nacional de Energía Atómica, Buenos Aires, Argentina
[c] Centro Atómico Bariloche, Comisión Nacional de Energía Atómica, Av. Bustillo 9500, 8400 Bariloche, Río Negro, Argentina
[d] Instituto de Física del Litoral, Universidad Nacional del Litoral – CONICET, Güemes 3450, 3000 Santa Fe, Argentina

ARTICLE INFO

Article history:
Received 25 October 2016
Accepted 16 December 2016
Available online 23 December 2016

Keywords:
Copper complex
Noncovalent interaction
Superexchange
EPR
Computational calculation

ABSTRACT

We report EPR and magnetic measurements of diaqua-(pyridine-2,6-dicarboxylato)Copper(II) together with computational calculations. This compound consists of an extended lattice of magnetically equivalent copper(II) ions in which the copper centers are linked by hydrophobic interactions such as π–π, π–metal, and Y–X...π, and hydrogen bonds involving different topologies, viz., —Cu—O_{eq}...O_{eq}—Cu—, —Cu—O_{eq}...O_{ap}—Cu—, and —Cu—O_{eq}...O=C—O_{eq}—Cu—. The powder EPR spectrum shows nearly axial symmetry with non-resolved hyperfine structure with the copper nucleus, suggesting the presence of intercenter isotropic exchange interactions. Single crystal EPR experiments show a single lorentzian resonance line for all the magnetic field orientations investigated, typical of an extended exchange coupled system. Susceptibility measurements showed weakly antiferromagnetically coupled Cu(II) ions ($J = -0.79$ (4) cm^{-1}). Using Anderson's exchange narrowing model for the collapse of the hyperfine structure, EPR yielded $|J| = 0.6$ (1) cm^{-1}. The distinct contributions of the different chemical pathways to the experimentally determined J-value are analyzed through first principle computational calculations.

1. Introduction

Hydrophobic and hydrogen bond interactions are noncovalent intermolecular forces that stabilize the structure of inorganic and organic compounds in condensed phase [1–5]. These interactions may also determine the magnetic behavior of solid state transition metal ion compounds, as these noncovalent bonds, when acting as linkers of paramagnetic molecular entities, may transmit from very weak ($J \approx 1\ cm^{-1}$) to relatively strong ($J \approx 100\ cm^{-1}$) exchange interactions ($H_{ex} = -J\ \mathbf{S}_1.\mathbf{S}_2$, also known as superexchange interaction) [6–11]. It is usually assumed that the very weak magnetic interactions do not determine the magnetic behavior of a given compound, but in some cases they may be responsible for magnetic anomalies observed in molecular magnets [12] and low dimensional magnetic materials [13]. J depends on the topology of the chemical pathway that transmits the exchange interaction and is related to the unpaired spin density delocalization along the chemical pathway that bridges the paramagnetic centers [14]. These characteristics serve to design materials with predictable properties such as molecular-based and single-molecule magnets [15–19]. Noncovalent interactions are also essential in biological systems such as redox enzymes and electron transfer proteins because, besides accomplishing structural roles [20], they may be involved in enzyme catalysis [21], molecular recognition [22], protein-substrate interaction [23], and chemical pathways in electron transfer reactions over large molecular distances [24,25]. Since these biomolecular pathways may in addition include paramagnetic centers coupled by exchange, determining J-values associated with them is relevant because the electron transfer rate is proportional to J [26,27].

Solid state copper(II) complexes are representative examples of exchange coupled systems which have extensively been investigated. Cu(II) ions present $S = 1/2$ spin, which makes them affordable to be studied from an experimental point of view by the two more appropriate techniques to evaluate exchange interactions: magnetic susceptibility measurements and electron paramagnetic resonance (EPR). The former is useful to evaluate J-values

* Corresponding author. Fax: +54 342 4575221.
E-mail address: brondino@fbcb.unl.edu.ar (C.D. Brondino).

http://dx.doi.org/10.1016/j.poly.2016.12.018
0277-5387/

above ~1 cm^{-1}, whereas the latter is better for $J < 1$ cm^{-1} [13,28–30]. Also, copper complexes present both a rich and a relatively simple chemistry, making it possible to obtain complexes with metal centers linked by different types of chemical bonds. For copper compounds, the role of covalent bonds in transmitting exchange interactions have profusely been documented [31–33], but much less for noncovalent interactions. The role of π-π interactions in copper complexes in transmitting exchange has experimentally been proven and is associated with very weak exchange interactions (<1 cm^{-1}) for nearly parallel aromatic rings even for interacting paramagnetic centers situated as far as 10 Å apart [34–38]. In contrast to π-π interactions, hydrogen bonds can transmit exchange with different strength depending on the bridge topology [10,39–41]. The interaction, which in most cases has been shown to be antiferromagnetic, is relatively strong for hydrogen bonds involving copper equatorial D (donor) and A (acceptor) ligands ($J = -21$ cm^{-1}), but diminishes considerably when one of the ligands is apical ($J = -7$ cm^{-1}) [10]. Less information exists for hydrogen bonds as superexchange pathways with D-A distances larger than 2.8 Å, though by extrapolating experimental and theoretical correlations J should be lower than 1 cm^{-1} for such large distances and hence hardly experimentally detectable by conventional magnetic measurements. Furthermore, it is common to find situations in which a combination of two or more noncovalent interactions appears in the molecular structure of the compounds. In those cases, it is not trivial to decide which pathway is the most relevant one to transmit superexchange, as the different pathways can interfere constructively to yield a maximum coupling or destructively to minimize it [42], or simply to accomplish merely a structural role [39,43]. This situation is analog to that found in redox metalloenzymes and electron transfer proteins, in which paramagnetic electron transfer centers may be bridged by more than one chemical pathway. Whether electron transfer in these cases is performed through only one of the possible *vias* or it is the result of a cooperative mechanism involving all the possible chemical paths is not clear up-to-date, but this is currently rationalized by computing the J value associated with each of the possible superexchange pathways connecting the centers [21].

With the objective in mind of analyzing how the electronic structure of paramagnetic centers linked by a multiple noncovalent chemical bridge is related to the efficiency of the individual potential superexchange pathways, we present here the magnetic properties of the copper complex diaqua-(pyridine-2,6-dicarboxylato) Copper(II) (hereafter CuDipic). The structure of the compound, which was reported elsewhere [44,45], shows copper centers linked by multiple hydrogen bonds and hydrophobic interactions. EPR measurements in powder, solution and oriented single crystal samples and magnetic measurements are used to evaluate the isotropic exchange coupling constant J between copper ions. The contribution of the individual chemical pathways linking copper ions to J is analyzed by computational calculations.

2. Materials and methods

All chemicals, of commercially available reagent grade, were used as received. The synthesis of the compound was performed as reported elsewhere [46]. Briefly, $CH_2Cu_2O_5$·(4 mmol, 0.221 g, Fluka) and dipicolinic acid (4 mmol, 0.167 g, Sigma) were dissolved in 200 mL of water, the solution was filtered using a 0.22 μm Millipore cellulose nitrate membrane and left to evaporate slowly at room temperature. After a few days blue-colored prismatic single crystals were obtained. The crystals were filtered, washed with a small amount of cold water, and dried under air. A word of caution: we would like to emphasise that single crystals are rather unstable out of the mother liquors, at ambient conditions. Upon removal from the solution they had to be characterized within a short period of time (~one week), after which they start a slow process of degradation.

The correctness of the phase obtained was confirmed by powder X-ray diffraction obtained on a Shimadzu XD-D1 diffractometer. This was needed because three different crystal phases of the compound can be found in the CSD. The phase herein described has been firstly reported by Sileo et al. [44], followed by a number of reports, on the same structure but of variable quality. In what follows we shall be using the results provided in what appears to be the best of these refinements [45]. The morphology of the single crystal, necessary to orient the sample for the EPR experiment, was determined by measuring the angles between crystal faces using a Carl Zeiss Axiolab goniometric microscope.

X-band CW-EPR spectra of oriented single crystals and powdered samples of CuDipic were obtained at room temperature on a Bruker EMX-Plus spectrometer, equipped with a rectangular cavity with 100 kHz field modulation. A single crystal of CuDipic was oriented by gluing its $(-1\,1\,0)$ face to a cleaved KCl cubic holder, which defined a set of orthogonal laboratory axes with the y direction corresponding to the crystal c axis (see Fig. S1 in Supplementary material). The cubic sample holder was placed on the top of a Rexolite® cylinder which was fitted to the end of a 4 mm OD quartz tube, as explained elsewhere [47]. The tube was positioned at the center of the microwave cavity and attached to a goniometer which allowed the sample to be rotated in 10° intervals with the magnetic field in the xy, zx and zy crystal planes of CuDipic. EPR spectra were analyzed with the EasySpin toolbox and homemade programs based on MATLAB [48].

The molar magnetic susceptibility $\chi(T)$ of the compound was measured between 1.8 and 100 K under an applied field of 500 Oe on a Quantum Design MPMS2 SQUID magnetometer using a calibrated gelatin capsule as sample holder with a small diamagnetic contribution. The values of the susceptibility were corrected for the diamagnetism of the constituent atoms using a value of -98.7×10^{-6} cm^3 mol^{-1} per molecular unit, obtained using Pascal's constants [49]. The contribution of the gelatin capsule was subtracted from the measured values.

The first-principle screened exchange hybrid density functional of Heyd, Scuseria, and Ernzerhof (HSE) with the basis set 6-311+G (d,p) was used to compute the energy of the antiferromagnetic (AF) and the ferromagnetic (F) states as implemented in GAUSSIAN suite of programs [50–52]. HSE functional was successfully used to predict the correct spin localization and the magnetic state of several systems [53,54]. The exchange coupling J is given by the difference in energy of the AF and F states, $\Delta E = (E_{AF} - E_F)$. In order to build the AF and F states we used the Fragment procedure implemented in GAUSSIAN [52].

This procedure to compute exchange coupling constants does not separate the different contributions of each chemical pathway in the case of a multiple path and must be considered as an effective coupling. The SCF convergence was achieved up to 10^{-9} Hartree (2×10^{-4} cm^{-1}). Calculations were based on the crystallographic structure, which includes the heavy atoms and also the hydrogen atoms, and no structural relaxation was allowed.

3. Results and discussion

3.1. Crystal and molecular structure

To facilitate the interpretation of the magnetic data, the EPR experiment, and computational calculations, we present first a brief description of the crystal structure. Full quantitative details can be obtained from the original structural reports [44,45]. The compound crystallizes in the triclinic system, space group $P\bar{1}$,

$Z = 2$ [45]. Fig. 1 shows distinct views of the molecular structure of CuDipic together with the labelling scheme used. The Cu(II) ions are in a nearly square pyramidal environment coordinated to two carboxylic oxygen atoms (O5 and O1), to one pyridine nitrogen, and to two oxygen atoms (O4 and O6) from water molecules (Fig. 1a). The 3D crystal lattice is composed of Cu(II) ions linked by different chemical pathways involving non-covalent interactions. Hydrophilic (H-bonds) and hydrophobic (π–π, Cu–π and CO–π) interactions are presented in Tables 1 and 2 with specific codes. The closest copper centers ($d_{Cu\text{-}Cu} = 4.724$ Å) are related by a [1 0 0] translation and are linked by two hydrogen bonds, viz., #1 (involving donor (D) and acceptor (A) atoms in equatorial positions) and #2, with D and A atoms in apical and equatorial positions, respectively. Among the different hydrophobic interactions linking these translationally related copper sites, the most relevant ones are quoted in Table 2, and can be described as π–π (Codes $1, $2), Cu–π (Code $3) and C—O…π (Codes #4 to #7) interactions (See Fig. 1b) [55]. The crystal structure is additionally stabilized by chemical pathways which involve hydrogen bonds and carboxylate groups of different topologies, viz. —Cu—$O6_{ap}$—H…O2=C—$O5_{eq}$—Cu— and —Cu—$O4_{eq}$—H…O3=C—$O1_{eq}$—Cu—, bridging copper centers related by an inversion (see Fig. 1c). The whole 3D packing of CuDipic is shown in Fig. 1d, in which the chemical pathways given above are additionally identified with the associated exchange coupling constants (J_1, #1 + #2 + $1–7; J_2, #4 + O=C—O—Cu; J_3, #3 + O=C—O—Cu).

3.2. Powder and frozen solution EPR measurements

The powder EPR spectrum of CuDipic at X-band (Fig. 2, spectrum a) shows a nearly axial symmetry ($g_{1,2,3} = 2.324$, 2.102, 2.043) with no evidences of hyperfine structure with the copper nucleus ($I = 3/2$), in line with a Cu(II) ion ($S = 1/2$) in a nearly square pyramidal coordination. The EPR spectrum of CuDipic dissolved in methanol shows a nearly axial symmetry with $g_{//,\perp} = 2.365$, 2.082 and $A_{//,\perp} = 124 \times 10^{-4}$, non-detectable cm^{-1} (Fig. 2, spectrum b). The $g_{//}$ and $A_{//}$ values in frozen methanolic solution are compatible with a copper ion in NO_3 nearly square planar coordination [56,57]. The difference in $g_{//}$ ($\Delta g = 0.04$) in both solid state and frozen solution may be indicating either a different nature for the apical ligand or a more regular coordination environment, with the latter being in line with the more axial EPR signal of the frozen solution. Both, the lack of hyperfine structure at $g_{//}$ in the solid state complex, the molecular orientation in which Cu(II) ions in square pyramidal coordination shows the maximal hyperfine splitting in absence of exchange interaction, and the low linewidth (2.8 mT at $g_{//}$) indicates the presence of Cu—Cu exchange interactions that collapse the hyperfine splitting into a single line [58,59].

3.3. Single crystal EPR measurements. the g-matrix

For a triclinic system consisting of an extended lattice of magnetically equivalent non-interacting Cu(II) ions ($S = 1/2$, $I = 3/2$), one would expect EPR spectra showing four hyperfine components for arbitrary magnetic field orientations relative to the molecular frame. In contrast, EPR spectra of CuDipic showed only one single resonance line with linewidths roughly constant in the range 1.27–1.45 mT (Fig. 2, lower panel; the full angular variation of both the spectra and linewidths are shown as Supplementary material in Figs. S2 and S3, respectively). The peak to peak linewidths are rather narrower than the expected ones for resonance lines broadened solely by magnetic dipole–dipole interactions, which confirms isotropic exchange interactions between Cu(II) ions.

To determine experimentally the ground state for the Cu(II) ion, we evaluated the components of the **g**-matrix associated with the Cu(II) ions of CuDipic. The positions of the single resonance lines were evaluated by least square fitting the derivative of a lorentzian function to the experimental spectra (Fig. S2) as reported elsewhere [47]. The angular variation of the square g-factor measured in the three crystal planes is shown in Fig. 3. The components of the g^2-matrix are given in Table 2 together with its eigenvalues and eigenvectors. The solid lines in Fig. 3, obtained using the g^2-matrix given in Table 2, are in good agreement with experiment.

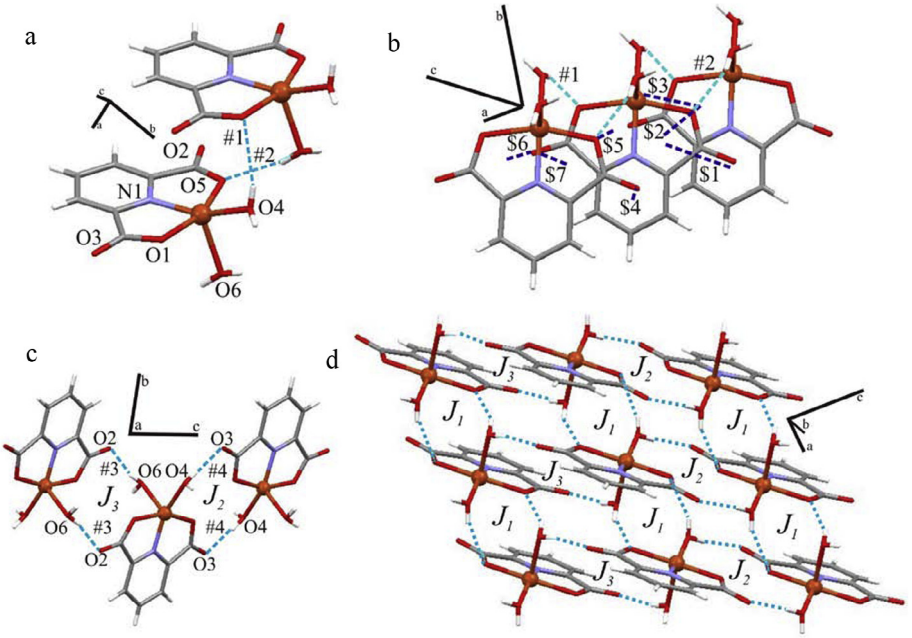

Fig. 1. (a) and (b) Coordination around the copper(II) ions showing the chemical pathways linking the closest metal centers related by [1 0 0] translations (c) Idem a y b but for the copper centers related by an inversion operation. (d) Perspective of the crystal unit cell showing the 3D arrangement of the copper centers. J_1, J_2, and J_3 are the isotropic exchange constants associated with the chemical pathways shown in a, b, and c and identified in Tables 1 and 2. Hydrogen bonds (coded with #) are indicated in dashed light blue lines, whereas hydrophobic interactions (coded with $) in dashed blue lines. (Color online.)

Table 1
Hydrogen bonding in CuDipic. Distances and angles are given in Å and degree, respectively.

D–H...A	D–H	H...A	D...A	∠DHA	D–A types	code
O4-H1...O1^{i}	0.76	2.31	2.976	147.8	eq-eq	#1
O6-H6...O5^{ii}	0.81	2.04	2.770	150.5	ap-eq	#2
O6-H4...O2^{iii}	0.73	2.02	2.731	166.2	ap-eq	#3
O4-H5...O3^{iv}	0.79	1.95	2.738	175.2	eq-eq	#4

Symmetry codes (i) x − 1, y, z; (ii) x + 1, y, z; (iii) −x, −y + 2, −z; (iv) −x + 1, −y + 2, −z + 1.

Table 2
Hydrophobic interactions in CuDipic. Distances and angles are given in Å and degree, respectively.

Interaction		Cg-Cg/X-Cg	β	γ	Code
π–π	Cg2...Cg3^{i}	3.9741(12)	37.4	37.0	$1
	Cg1...Cg2^{ii}	3.5432(12)	26.7	28.4	$2
π-metal	Cu...Cg1^{i}	3.878	34.24		$3
Y–X...π	C1-O2...Cg3^{i}	3.231(2)		4.5	$4
	C1-O5...Cg1^{i}	3.113(2)		5.0	$5
	C4-O3...Cg1^{ii}	3.201(2)		18.24	$6
	C4-O3...Cg2^{ii}	3.312(2)		23.54	$7

β = Angle Cg(***m***)–Cg(***n***) or Cg(***m***) → Cu vector and normal to plane ***m*** (°); **γ** = Angle Cg(***m***) → Cg(***n***) vector and normal to plane ***n*** (°); **Cg–Cg** = Distance between ring Centroids (Å). Symmetry codes (i) x − 1, y, z; (ii) x + 1, y, z.

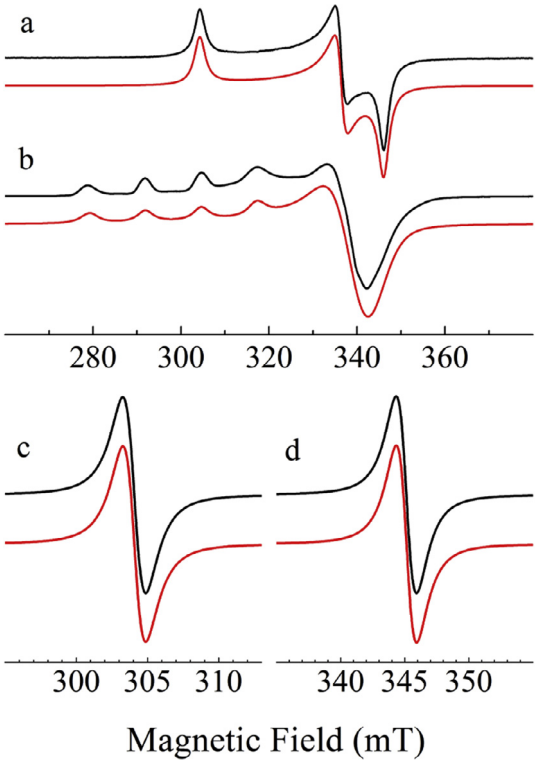

Fig. 2. *Upper panel:* Powder (a) and frozen solution (b) EPR spectra of CuDipic taken at 9.876 GHz and 120 K together with simulation (red lines). The EPR parameters used in simulation were $g_{1,2,3}$ = 2.324, 2.102, 2.043 for the powder spectrum and $g_{//,\perp}$ = 2.365, 2.082, $A_{//,\perp}$ = 124 × 10^{-4} cm^{-1}, non-detectable for the solution spectrum. The room temperature EPR powder spectrum is similar to that at 120 K. *Lower Panel:* Single crystal EPR spectra for magnetic field orientations approximately lying along the g_1 (c) and g_3 (d) directions. Simulations (red lines) were performed with eq. under Section 3.4. (Color online.)

The fact that the eigenvalues obtained from single crystal EPR spectroscopy are in good agreement with those obtained from powder spectral EPR simulation (Fig. 2, spectrum a) confirms that the EPR powder spectrum corresponds to that of single Cu(II) ions in which the hyperfine multiplet is collapsed by exchange interactions. Both, the eigenvalues (Table 3, $g_1 > g_2 \sim g_3$) and the eigenvector orientation relative to the molecular frame (Fig. 4) confirm a ground state determined mainly by a d_{x2-y2} type orbital, in line with the computational calculations given below.

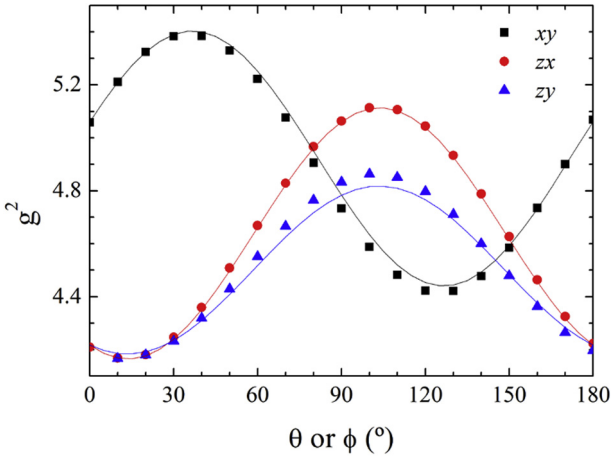

Fig. 3. Angular variation of $g^2(\theta,\phi)$ in three crystal planes of CuDipic. θ and ϕ are the polar and azimuthal angles, respectively in the *xyz* system. The relation between the lab *x, y, z* axes system and the crystal axes system is shown in Fig. S1.

3.4. Exchange interaction evaluated by EPR and magnetic measurements

We evaluated the isotropic exchange interaction that couples the Cu(II) ions of CuDipic by EPR using a method based on the Anderson's model of exchange narrowing [60,61]. In this theory,

Table 3
Components, eigenvalues, and eigenvectors of the crystal g^2-matrix of CuDipic in the experimental *xyz* coordinate system.

g^2_{xx} = 5.061(6)	g^2_{xy} = 0.461(7)
g^2_{yy} = 4.783(6)	g^2_{zx} = −0.218(7)
g^2_{zz} = 4.218(6)	g^2_{zy} = −0.143(7)
g_1 = 2.336(9)	**a**$_1$ = [-0.787(3), 0.582(4), 0.205(5)]
g_2 = 2.107(8)	a$_2$ = [0.585(7), −0.810(4), −0.05(3)]
g_3 = 2.040(3)	**a**$_3$ = [0.20(2), 0.08(2), 0.977(2)]

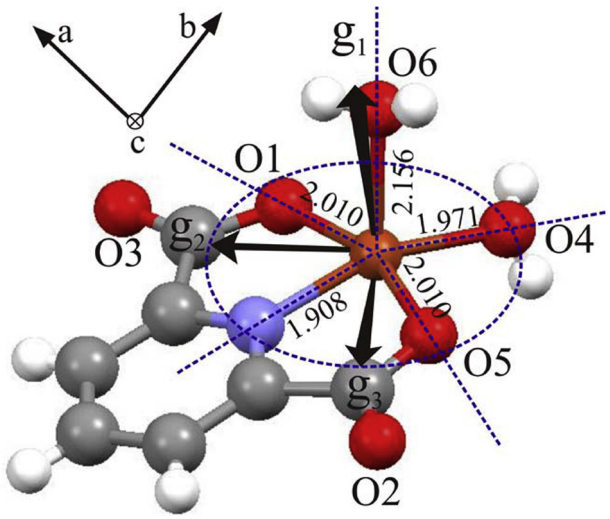

Fig. 4. **g**-matrix orientation for the Cu(II) ion of CuDipic in the molecular frame.

the absorption spectrum in the frequency domain for an extended lattice of paramagnetic centers coupled by a unique exchange interaction is given by [62]

$$I(\omega;\omega_e) = \mathrm{Re}\{\mathbf{W}\cdot[i(\boldsymbol{\omega}-\omega\mathbf{E}+i\boldsymbol{\Gamma})+\boldsymbol{\pi}]^{-1}\cdot\mathbf{1}\}$$

where ω is the microwave frequency, ω_e is the exchange frequency ($\omega_e \approx J/\hbar$), **W** is a vector whose components are intensities of the resonance lines to be collapsed by exchange, $\boldsymbol{\omega}$ and $\boldsymbol{\Gamma}$ are diagonal matrices whose elements are the absorption frequencies ω_i ($\omega_i = g\mu_B B_i/\hbar$; B_i = position in magnetic field units of the resonance line) and linewidths Γ_i in the absence of exchange and any broadening interaction, respectively, $\boldsymbol{E}$ is the unit matrix, and $\boldsymbol{\pi}$ is a matrix with elements proportional to ω_e that give the transition probabilities between the distinct resonance lines, and **1** is a vector with all components equal to one.

The single crystal experiment of CuDipic shows single exchange collapsed resonance lines with almost constant linewidth (see Fig. 2 lower panel and Fig. S3), indicating a situation of strong exchange ($\omega_e >> A_{iso}/\hbar$). Resolution of eq for $I(\omega, \omega_e)$ (see above) for CuDipic requires the determination of the ω_i positions and the Γ_i linewidths [63,64]. ω_i positions in the $g_{//}$ region were estimated using the $A_{//}$ hyperfine parameter obtained from the solution spectra ($\omega_i = g_{//}\mu_B B_{//}/\hbar + m_I A_{//}/\hbar$, $m_I = 3/2,1/2,-1/2,-3/2$). An experimental estimation of the Γ_i linewidths is more difficult, as even in the case of the solution spectra, nonresolved hyperfine couplings with copper ligands nuclei contribute to the linewidth. However, solution of eq $I(\omega, \omega_e)$ under the conditions $\omega_e >> A_{iso}/\hbar$ yields a single line with position at the gravity center of the hyperfine multiplet and linewidth Γ_i for any magnetic field orientation, which means that the intrinsic linewidth of the copper resonances can be obtained from single crystal EPR experiments in copper compounds under conditions of strong exchange. Considering a linewidth ~8 G from single crystal EPR experiments of Cu(II) complexes strongly coupled by exchange, simulation with equation $I(\omega, \omega_e)$ to the experimental spectra (Fig. 2 lower panel) yielded $|J| = 0.6\ (1)\ cm^{-1}$. The relatively large uncertainty of this result is due to the lack of sensitivity of EPR to evaluate J values of the order of 1 cm^{-1} or larger, as they do not produce significant narrowing of the linewidth.

Magnetic susceptibility measurements showed a Curie–Weiss behavior in the range temperature 1.8–100 K. Least squares fitting of the inverse of the susceptibility vs T yielded $C = 0.391\ (1)$ emuK/mol typical of mononuclear Cu(II) ions and $\theta = -0.59\ (3)$ K (Fig. 5). At lower temperature a pronounced decrease of the product χT vs T (inset on the Figure) typical of weak antiferromagnetic interactions between copper ions is observed. Taking into account the θ obtained and considering four neighbors for each copper center as observed crystallographically we would evaluate $J = -0.59\ (4)\ cm^{-1}$ using the molecular field theory [49]. However, as discussed below in Section 3.5, each copper center is surrounded only by three magnetically coupled neighbors, which yielded $J = -0.79\ (4)\ cm^{-1}$.

3.5. Computational calculations

Calculations were performed to rationalize the experimentally determined isotropic exchange constant assuming isolated copper dimeric units coupled by J_1, J_2, and J_3 (Fig. 1). The system was modelled as follows: two consecutive monomers translated along the *a*-axis, which are linked by hydrogen bond interactions #1 and #2 and hydrophobic interaction $1–7 (Table 1 and Fig. 1), to compute J_1; two consecutive monomers related by an inversion, which are connected by hydrogen bonds #4, to compute J_2; two adjacent monomers, as before, connected by hydrogen bonds #3 to compute J_3.

For all these models calculations indicated a ground state corresponding to spins antiferromagnetically coupled with $J_1 = -0.12\ cm^{-1}$, $J_2 = -0.11\ cm^{-1}$ and $J_3 \leqslant -0.01\ cm^{-1}$. The small value for J_3 (hydrogen bonds #3 + carboxylate group) relative to J_1 and J_2 is in line with the fact that H-bond bridges involving –Cu-O6$_{ap}$—H…O2=C—O5$_{eq}$—Cu— transmit weaker exchange interactions than those implying an equatorial one [10]. Within this scheme of exchange pathways, we propose that each copper center is mainly coupled by exchange to three neighbors, two of them at 4.724 Å (Cu(II) ions coupled by J_1 (Fig. 1a and b), whereas the third one at 5.802 Å (Cu(II) ions coupled by J_2) (Fig. 1d). Hence, the 3D structural lattice of CuDipic would behave as a ladder-like structure from a magnetic point of view, where the ladder legs are determined by J_1 and the rungs by J_2 [65]. Though the angular variation of the linewidth shown in Fig. S3 resembles the one expected for a 1D magnetic behavior [66], the remarkably isotropic linewidth does not allow us to extract a clear experimental evidence for reinforcing the 1D magnetic behavior predicted by calculations.

3.6. Contribution of the individual chemical pathways to the exchange interaction

We further evaluated by computational methods the contribution of the individual chemical pathways to J_1 and J_2 using the

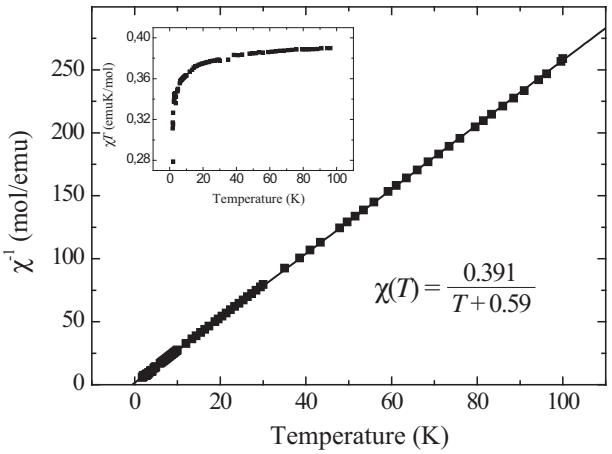

Fig. 5. Plot of the inverse of the magnetic susceptibility $\chi^{-1}(T)$ *vs* T for CuDipic. The magnetic data are corrected for diamagnetism as explained in the text (See Material and Methods). The inset displays the values of χT *vs* T. The values of constants obtained following a Curie–Weiss model are also indicated.

Table 4
Calculated exchange coupling constants obtained upon selective structural modifications of the bridging chemical pathways associated with the exchange parameter J_1 (Fig. 1a and b). The exchange coupling constant obtained without structural modifications is also given for comparison. The chemical pathways are indicated according to the codes given in Table 2. The atomic coordinates of the artificially modified structures are given in the Supplementary material (Table S1). The omitted code indicates the artificially modified chemical pathway.

Chemical Pathways #1: $O4_{eq}$—H1...$O1_{eq}$ #2: $O6_{ap}$-H6...$O5_{eq}$ $1-7: π–π, Cu–π and CO–π	modified structural parameter		J_1 value (cm^{-1})
	H coordinates	interplanar dipic separation	
#1 + #2 + $1–7	As the crystal structure	As the crystal structure	−0.12
#2 + $1–7	See supplementary material		−0.15
#1 + $1–7			−0.12
$1–7			−0.16
#1 + #2		−0.02 Å	−0.29
		−0.04 Å	−0.68
		+0.02 Å	−0.05

above discussed dimeric model in which the linking chemical pathways were artificially modified (Fig. 1a, b and c). The hydrogen bond interactions were modified by rotating the H_2O molecule keeping fixed in position the O atom and varying the H positions, keeping unchanged the rest of the molecule. The effect of the hydrophobic interactions on J_1 was evaluated by modifying the separation between interacting Dipic rings by displacing them along the *a* crystal axis without producing a significant structural distortions in the hydrogen bond network. The J_1 values obtained with this procedure are summarized in Table 4. As shown in this table, decreasing the interplanar Dipic separation relative to the position determined crystallographically yielded higher J_1 values, whereas negligible J values within the error limit of the theory used in the computational method are obtained upon increasing the separation. In contrast, hydrogen bond modifications do not show significant changes in J; it produces a small increasing of J when the hydrogen bond #1 is quenched whereas the quenching of #2 yielded approximately the same J-value. These results altogether confirmed that the exchange interaction J_1 is mainly governed by the hydrophobic interaction with a small contribution of hydrogen bond coded #1. The magnitude of the exchange transmitted by the hydrophobic interactions studied here is one order of magnitude larger than in copper compounds containing phenanthroline ligands as superexchange paths [35,59,64], which is consistent with both the shorter Cu—Cu distance in CuDipic and the higher spin density on the aromatic ligand atoms (see below), compared with these complexes. On the other hand, J_2 which is determined by the double symmetrical hydrogen bonds coded #4 plus a carboxylate group, decreased to a value within the error limit of the theory used when only one hydrogen bond of the double bridge was modified. This result is consistent with theoretical work which indicates that symmetrical double chemical pathways interfere constructively to the J value [42].

Finally, we analyzed the relationship between unpaired spin density on each magnetic center and the exchange coupling constants on the basis of the qualitative Khan's model for dimeric systems [14]. In this model, the coupling constant is proportional to the overlap density in the bridging pathway between the two metal centers, $\rho(i) = \phi_1(i)\,\phi_2(i)$, where ϕ_1 and ϕ_2 are the magnetic orbitals of the two interacting copper centers and i identifies the unpaired electrons. Thus, the larger the unpaired spin delocalization towards the bridging ligands, the larger the exchange interaction. Calculations performed on Cu(II) centers coupled by J_1 or J_2 show that for both cases ~63% of the unpaired spin density on each monomer is localized on the Cu(II) ion (Fig. 6), in line with EPR results. The remaining 37% is asymmetrically delocalized towards the copper ligands (N, ~14%; O1, ~12%; O5, ~7%; O4 2,2%; O6, negligible). Similar unpaired spin densities were found for the isolated monomer, indicating that the unpaired spin delocalization is determined mainly by the first coordination sphere ligands of the metal ion. This is showing that, in addition to the topology of a given chemical pathway, the anisotropy in the unpaired spin density is essential to determine the superexchange pathway in paramagnetic compounds presenting multiple chemical pathways with potential capability to transmit exchange.

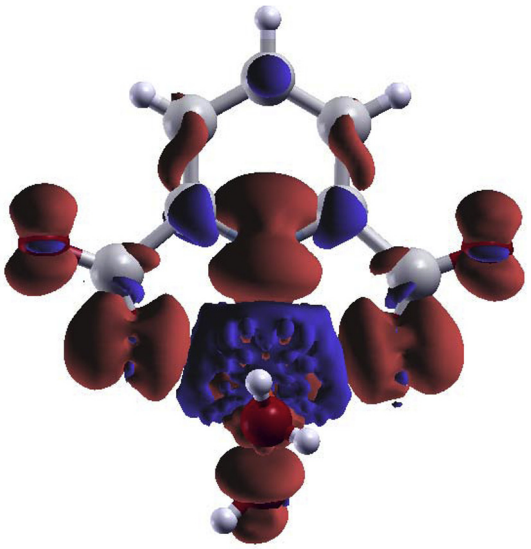

Fig. 6. Mulliken spin densities computed for the antiferromagnetic state for the structure of CuDipic (0.005 e^-). The blue and the red colors identify the spin state. The apical water molecule shows negligible spin density compared with the other copper ligands. (Color online.)

4. Conclusions

CuDipic shows Cu(II) ions linked by multiple non covalent interactions involving hydrogen bonds with D-A distances >2.7 A and hydrophobic interactions of the π–π, Cu–π and CO–π types. EPR studies together with magnetic measurements allowed us to conclude that the Cu(II) ions are very weakly antiferromagnetically coupled by isotropic exchange mediated by these non-covalent interactions. Computational calculations indicated that the sign and magnitude of the exchange interaction is mainly determined by the hydrophobic interactions and the mixed chemical pathways involving a H-bond (#4) plus a carboxylate group. The results also confirm that hydrogen bonds with D-A distances larger than 2.9 Å (#1), in which D and A are equatorial ligands to copper, are not capable of transmitting significant superexchange interactions, accomplishing mainly a structural role.

This paper shows that a given multiple chemical bridge, here hydrophobic interactions and hydrogen bonds, may provide different superexchange pathways depending on the unpaired spin density delocalized on the ligands of the metal center; in other words, the ligand environment around the metal centers determines the superexchange pathway. Since the chemical pathways studied here show some resemblance with those present in redox metalloenzymes and electron transfer proteins in which the electron transfer rate is directly related to the isotropic exchange constant, these results can be helpful to answer the question of why electron transport prefers one chemical pathway over the others.

Acknowledgments

This work was supported by FONCyT, CONICET, and CAI+D-UNL. A.L.P. thanks CONICET for a fellowship grant. N.I.N., S.D.D. and C.D. B. are members of CONICET-Argentina.

Appendix A. Supplementary data

Supplementary data associated with this article can be found, in the online version, at http://dx.doi.org/10.1016/j.poly.2016.12.018.

References

[1] T. Steiner, Angew. Chem. Int. Ed. 41 (1) (2002) 48.
[2] L. Brammer, J.C.M. Rivas, R. Atencio, S. Fang, F.C. Pigge, Dalton Trans. 21 (2000) 3855.
[3] C.A. Hunter, J.K.M. Sanders, J. Am. Chem. Soc. 112 (14) (1990) 5525.
[4] A.S. Mahadevi, G.N. Sastry, Chem. Rev. 113 (3) (2013) 2100.
[5] M. Atzori, A. Serpe, P. Deplano, J.A. Schlueter, M. Laura Mercuri, Inorg. Chem. Front. 2 (2) (2015) 108–115.
[6] B.A. Zurowska, Inorg. Chim. Acta 418 (2014) 136–152.
[7] T. Cauchy, E. Ruiz, O. Jeannin, M. Nomura, M. Fourmigué, Chem. Eur. J. 13 (31) (2007) 8858.
[8] C.P. Constantinides, P.A. Koutentis, J.M. Rawson, Chem. Eur. J. 18 (48) (2012) 15433.
[9] M. Peric, M. Zlatar, S. Grubisic, M. Gruden-Pavlovic, Polyhedron 42 (1) (2012) 89.
[10] W. Plass, A. Pohlmann, J. Rautengarten, Angew. Chem. Int. Ed. 40 (22) (2001) 4207.
[11] G. De Munno, D. Viterbo, A. Caneschi, F. Lloret, M. Julve, Inorg. Chem. 33 (8) (1994) 1585.
[12] M.V. Fedin, S.L. Veber, K.Y. Maryunina, G.V. Romanenko, E.A. Suturina, N.P. Gritsan, R.Z. Sagdeev, V.I. Ovcharenko, E.G. Bagryanskaya, J. Am. Chem. Soc. 132 (39) (2010) 13886.
[13] R.A. Allao, A.K. Jordao, J.A.L.C. Resende, A.C. Cunha, V.F. Ferreira, M.A. Novak, C. Sangregorio, L. Sorace, M.G.F. Vaz, Dalton Trans. 40 (41) (2011) 10843.
[14] O. Kahn, Angew. Chem. Int. Ed. Engl. 24 (10) (1985) 834.
[15] M. Castellano, R. Ruiz-García, J. Cano, J. Ferrando-Soria, E. Pardo, F.R. Fortea-Pérez, S.E. Stiriba, M. Julve, F. Lloret, Acc. Chem. Res. 48 (3) (2015) 510.
[16] F. Meyer, S. Demeshko, G. Leibeling, B. Kersting, E. Kaifer, H. Pritzkow, Chem. Eur. J. 11 (5) (2005) 1518.
[17] E. Moreno Pineda, N.F. Chilton, R. Marx, M. Dörfel, D.O. Sells, P. Neugebauer, S.-D. Jiang, D. Collison, J. van Slageren, E.J.L. McInnes, R.E.P. Winpenny, Nat. Commun. 5 (2014) 5243.
[18] J. Camarero, E. Coronado, J. Mater. Chem. 19 (12) (2009) 1678.
[19] D. Cangussu, E. Pardo, M.-C. Dul, R. Lescouëzec, P. Herson, Y. Journaux, E.F. Pedroso, C.L.M. Pereira, H.O. Stumpf, M. Carmen Muñoz, R. Ruiz-García, J. Cano, M. Julve, F. Lloret, Inorg. Chim. Acta 361 (12–13) (2008) 3394.
[20] M.J. Plevin, D.L. Bryce, J. Boisbouvier, Nat. Chem. 2 (6) (2010) 466.
[21] R.G. Hadt, S.I. Gorelsky, E.I. Solomon, J. Am. Chem. Soc. 136 (42) (2014) 15034.
[22] C.L. Perrin, J.B. Nielson, Annu. Rev. Phys. Chem. 48 (1) (1997) 511.
[23] M.J. Romao, C.A. Cunha, C.D. Brondino, J.J. Moura, Met. Ions Biol. Syst. 39 (2002) 539.
[24] C.C. Moser, J.L.R. Anderson, P.L. Dutton, Biochim. Biophys. Acta Bioenergetics 1797 (9) (2010) 1573.
[25] H.B. Gray, J.R. Winkler, Biochim. Biophys. Acta Bioenergetics 1797 (9) (2010) 1563.
[26] R. Calvo, R.A. Isaacson, M.L. Paddock, E.C. Abresch, M.Y. Okamura, A.L. Maniero, L.C. Brunel, G. Feher, J. Phys. Chem. B. 105 (19) (2001) 4053.
[27] M. Gómez, N. Neuman, S. Dalosto, P. González, J.G. Moura, A. Rizzi, C. Brondino, J. Biol. Inorg. Chem. 20 (2) (2015) 233.
[28] A.C. Rizzi, N.I. Neuman, P.J. González, C.D. Brondino, Eur. J. Inorg. Chem. 2 (2016) 192.
[29] A. Bencini, C. Benelli, D. Gatteschi, C. Zanchini, J. Am. Chem. Soc. 106 (20) (1984) 5813.
[30] S.L. Veber, M.V. Fedin, A.I. Potapov, K.Y. Maryunina, G.V. Romanenko, R.Z. Sagdeev, V.I. Ovcharenko, D. Goldfarb, E.G. Bagryanskaya, J. Am. Chem. Soc. 130 (8) (2008) 2444.
[31] A. Banerjee, R. Singh, E. Colacio, K.K. Rajak, Eur. J. Inorg. Chem. 2 (2009) 277.
[32] A. Mukherjee, I. Rudra, S.G. Naik, S. Ramasesha, M. Nethaji, A.R. Chakravarty, Inorg. Chem. 42 (18) (2003) 5660.
[33] P.R. Levstein, R. Calvo, Inorg. Chem. 29 (8) (1990) 1581.
[34] C.D. Brondino, R. Calvo, A.M. Atria, E. Spodine, O. Peña, Inorg. Chim. Acta 228 (2) (1995) 261.
[35] N.I. Neuman, M. Perec, P.J. González, M.C.G. Passeggi, A.C. Rizzi, C.D. Brondino, J. Phys. Chem. A 114 (50) (2010) 13069.
[36] V. Voronkova, R. Galeev, L. Korobchenko, A.M. Madalan, M. Andruh, V.C. Kravtsov, Y.A. Simonov, App. Magn. Reson. 28 (3–4) (2005) 297.
[37] D. Venegas-Yazigi, K.A. Brown, A. Vega, R. Calvo, C. Aliaga, R.C. Santana, R. Cardoso-Gil, R. Kniep, W. Schnelle, E. Spodine, Inorg. Chem. 50 (22) (2011) 11461.
[38] Y.-H. Chi, J.-M. Shi, H.-N. Li, W. Wei, E. Cottrill, N. Pan, H. Chen, Y. Liang, L. Yu, Y.-Q. Zhang, C. Hou, Dalton Trans. 42 (44) (2013) 15559.
[39] P. Talukder, S. Sen, S. Mitra, L. Dahlenberg, C. Desplanches, J.-P. Sutter, Eur. J. Inorg. Chem. 2 (2006) 329.
[40] C. Desplanches, E. Ruiz, A. Rodríguez-Fortea, S. Alvarez, J. Am. Chem. Soc. 124 (18) (2002) 5197.
[41] F. Nepveu, S. Gehring, L. Walz, Chem. Phys. Lett. 128 (3) (1986) 300.
[42] P.R. Levstein, H.M. Pastawski, J.L.D. Amato, J. Phys.: Condens. Matter 2 (7) (1990) 1781.
[43] N.A.G. Bandeira, D. Maynau, V. Robert, B. Le Guennic, Inorg. Chem. 52 (14) (2013) 7980.
[44] E.E. Sileo, G. Rigotti, B.E. Rivero, M.A. Blesa, J. Phys. Chem. Solids 58 (7) (1997) 1127.
[45] R. Gupta, S. Sanotra, H.N. Sheikh, B.L. Kalsotra, V.K. Gupta, Rajnikant, J. Coord. Chem. 65 (22) (2012) 3917.
[46] E.E. Sileo, M.F. Quinteros-Rivero, B.E. Rivero, G. Rigotti, M.A. Blesa, Solid State Ion. 73 (1–2) (1994) 153.
[47] J.M. Schveigkardt, A.C. Rizzi, O.E. Piro, E.E. Castellano, R. Costa de Santana, R. Calvo, C.D. Brondino, Eur. J. Inorg. Chem. 11 (2002) 2913.
[48] S. Stoll, A. Schweiger, J. Magn. Reson. 178 (1) (2006) 42.
[49] O. Kahn, Molecular Magnetism, VCH Publishers, New York, 1993.
[50] J. Heyd, G.E. Scuseria, M. Ernzerhof, J. Chem. Phys. 118 (18) (2003) 8207.
[51] J. Heyd, G.E. Scuseria, M. Ernzerhof, J. Chem. Phys. 124 (2006) 21.
[52] M.J. Frisch, G.W. Trucks, H.B. Schlegel, G.E. Scuseria, M.A. Robb, J.R. Cheeseman, G. Scalmani, V. Barone, B. Mennucci, G.A. Petersson, H. Nakatsuji, M. Caricato, X. Li, H.P. Hratchian, A.F. Izmaylov, J. Bloino, G. Zheng, J.L. Sonnenberg, M. Hada, M. Ehara, K. Toyota, R. Fukuda, J. Hasegawa, M. Ishida, T. Nakajima, Y. Honda, O. Kitao, H. Nakai, T. Vreven, J. Montgomery, J. A., J.E. Peralta, F. Ogliaro, M. Bearpark, J.J. Heyd, E. Brothers, K.N. Kudin, V.N. Staroverov, R. Kobayashi, J. Normand, K. Raghavachari, A. Rendell, J.C. Burant, S.S. Iyengar, J. Tomasi, M. Cossi, N. Rega, J.M. Millam, M. Klene, J.E. Knox, J.B. Cross, V. Bakken, C. Adamo, J. Jaramillo, R. Gomperts, R.E. Stratmann, O. Yazyev, A.J. Austin, R. Cammi, C. Pomelli, J.W. Ochterski, R.L. Martin, K. Morokuma, V.G. Zakrzewski, G.A. Voth, P. Salvador, J.J. Dannenberg, S. Dapprich, A.D. Daniels, O. Farkas, J.B. Foresman, J.V. Ortiz, J. Cioslowski, D.J. Fox, Gaussian 09, Revision C.1. Gaussian Inc, Wallingford CT (2009).
[53] J.L.F. Da Silva, M.V. Ganduglia-Pirovano, J. Sauer, V. Bayer, G. Kresse, Phys. Rev. B 75 (4) (2007) 045121.
[54] I.D. Prodan, G.E. Scuseria, R.L. Martin, Phys. Rev. B 76 (3) (2007) 033101.
[55] C. Janiak, Dalton Trans. 21 (2000) 3885.
[56] R. Calvo, C.A. Steren, O.E. Piro, T. Rojo, F.J. Zuniga, E.E. Castellano, Inorg. Chem. 32 (26) (1993) 6016.
[57] C.D. Brondino, N.M.C. Casado, M.C.G. Passeggi, R. Calvo, Inorg. Chem. 32 (10) (1993) 2078.
[58] C.D. Brondino, R. Calvo, E.J. Baran, Chem. Phys. Lett. 271 (1–3) (1997) 51.
[59] N.I. Neuman, V.G. Franco, F.M. Ferroni, R. Baggio, M.C.G. Passeggi, A.C. Rizzi, C. D. Brondino, J. Phys. Chem. A 116 (50) (2012) 12314.
[60] P.W. Anderson, J. Phys. Soc. Jpn. 9 (3) (1954) 316.
[61] P.W. Anderson, P.R. Weiss, Rev. Mod. Phys. 25 (1) (1953) 269.
[62] R.A. Sack, Mol. Phys. 1 (2) (1958) 163.
[63] C.D. Brondino, R. Calvo, A.M. Atria, E. Spodine, O.R. Nascimento, O. Peña, Inorg. Chem. 36 (14) (1997) 3183.
[64] N.I. Neuman, E. Burna, R. Baggio, M.C.G. Passeggi, A.C. Rizzi, C.D. Brondino, Inorg. Chem. Front. 2 (9) (2015) 837.
[65] T. Barnes, J. Riera, Phys. Rev. B 50 (10) (1994) 6817.
[66] A. Bencini, D. Gatteschi, Electron Paramagnetic Resonance of Exchange Coupled Systems, Springer-Verlag, Berlin, Germany, 1990.